# Adaptive Optimal Tracking Control for a Flywheel Energy Storage System without the Use of a Model

**Thi Thanh Hoa Lai**
Thai Nguyen University of Technology, Vietnam
laithithanhhoa@tnut.edu.vn (corresponding author)

**Hai Do Trung**
Thai Nguyen University of Technology, Vietnam
dotrunghai@tnut.edu.vn

**K. L. Lai**
Thai Nguyen University of Technology, Vietnam
laikhaclai@tnut.edu.vn

*Received: 5 April 2025 | Revised: 4 May 2025 and 22 May 2025 | Accepted: 31 May 2025*

 *DOI: https://doi.org/10.48084/etasr.11299*

**ABSTRACT**

**This study presents an adaptive optimal tracking control method for a Flywheel Energy Storage System (FESS) using an Induction Motor (IM) without requiring an accurate system model. The control system employs a Deep Neural Network (DNN) identifier combined with an optimal controller and a Critic Neural Network (CNN) to ensure that the FESS output power follows the reference power value. The simulation results demonstrate that the proposed method achieves high accuracy and strong self-adaptation to system variations.**

***Keywords-deep neural network; IM-FESS; optimal control; dynamic control; dynamic neural network***

## I. INTRODUCTION

The development of renewable energy sources, such as solar and wind power, brings significant benefits, but also poses major challenges in terms of power intermittency and volatility. These issues greatly affect the stability and power quality of an electrical grid system. The FESS is an effective solution to balance power, regulate frequency, and stabilize the grid. FESS operates by converting the electrical energy into mechanical energy in the form of rotational kinetic energy and can return the energy in the form of electricity instantly when needed [1, 2].

Two common types of electric machines used in FESS are the Permanent Magnet Synchronous Machines (PMSMs) and Induction Machines (IMs) [2-4], forming systems known as PMSM-FESS and IM-FESS. Extensive research has been conducted on controlling PMSM-FESS [5-7]. However, controlling IM-FESS is a complex problem due to the system's nonlinearity and uncertainties, particularly when it exhibits non-affine characteristics, saturation effects, and time-varying parameters in the IM and power electronics converter. These factors result in inaccurate or incomplete mathematical models, making it difficult to design an optimal controller.

Classical control methods, such as the PID control [8-10] or state feedback control [11], require an accurate mathematical model of the system. However, since FESS is a nonlinear system with varying parameters and disturbances, the PID control often fails to guarantee high performance under all operating conditions. Advanced control methods, such as backstepping optimal control [12] are designed to minimize an objective function (e.g., energy dissipation, power deviation) [12]. However, this approach relies heavily on an accurate mathematical model of the system, making it challenging to apply when FESS exhibits non-affine properties. Model Predictive Control (MPC) [13] and $H_2/H_\infty$ robust control [14] are powerful methods for handling constraints and real-time optimization. However, MPC requires an accurate dynamic model, and when the system is subjected to disturbances, parameter variations, or uncertainties, this method tends to experience performance degradation.

To address these challenges, this study proposes an adaptive optimal tracking control method for non-affine FESS without using a model. The goal is to introduce a novel control architecture that integrates a CNN and a DNN identifier to learn the system dynamics without requiring an accurate mathematical model. The proposed adaptive optimal control

mechanism enables the system to track the reference power $P_{ref}(t)$, despite the parameter variations and disturbances. This ensures that the system operates according to the desired standards without needing an accurate mathematical model of FESS. The stability analysis of the system is conducted based on the Lyapunov method. The proposed control method is evaluated through simulations in MATLAB/Simulink.

## II. MATHEMATICAL MODEL OF IM-FESS CONSIDERING SATURATION, PARAMETER VARIATIONS AND LOAD DISTURBANCES

The IM-FESS is an energy storage solution based on the principle of conserving the rotational momentum. When excess energy is available in the power system, FESS converts the electrical energy into mechanical energy by accelerating the flywheel. Conversely, when additional energy is required, FESS releases the stored energy by decelerating the flywheel and converting kinetic energy back into electrical energy. As shown in Figure 1, the standard FESS consists of the following main components:

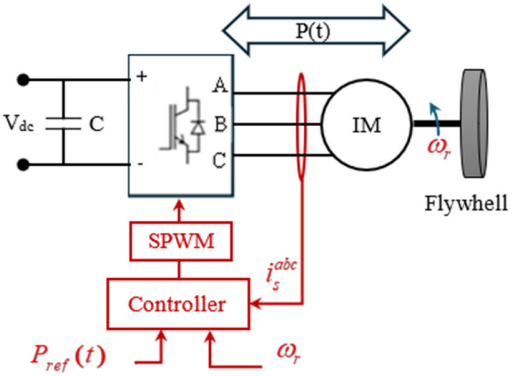


Fig. 1. IM-FESS block diagram.

- Flywheel: A rotating mass that stores energy in the form of kinetic energy.
- IM: Operates in both motor mode (charging) and generator mode (discharging).
- Power converter: Controls the current and voltage to manage the charging/discharging process.
- Controller: This ensures that the output power of the FESS follows the reference power $P_{ref}$.

The mathematical model of the IM-FESS, considering the load variation, magnetic saturation, and parameter uncertainty, in a standard decoupled matrix form can be written as [14]:

$$\dot{x} = Ax + Bu \quad (1)$$

in which the state vector is:

$$x = [i_{ds} \quad i_{qs} \quad i_{dr} \quad i_{qr} \quad \omega_r]^T \quad (2)$$

and the control vector (stator voltage) is:

$$u = [v_{sd} \quad v_{sq}]^T \quad (3)$$

The matrix A, considering load disturbance, magnetic saturation (nonlinearity), and parameter uncertainty, is:

$$A = A_0 + \sum_{i=1}^{3} \Delta_i A_i, \quad |\Delta_i| \le 1 \quad (4)$$

where $A_0$ is the nominal state matrix, $A_1$ accounts for the load variations, $A_2$ represents the effects of magnetic saturation, and $A_3$ captures the parameter uncertainties. The term $\Delta_i A_i$ represents the disturbances, nonlinearities, or the influence of varying loads.

The nominal state matrix is derived from the electromagnetic equations of the IM, which can be expressed as [6]:

$$A_0 = \begin{bmatrix} -\frac{R_s}{L_s} & \omega_s & -\frac{L_m}{L_s L_r}R_r & 0 & 0 \\ -\omega_s & -\frac{R_s}{L_s} & 0 & -\frac{L_m}{L_s L_r}R_r & 0 \\ \frac{L_m}{L_r}R_s & 0 & -\frac{R_r}{L_r} & \omega_r & 0 \\ 0 & \frac{L_m}{L_r}R_s & -\omega_r & -\frac{R_r}{L_r} & 0 \\ \frac{3}{2}\frac{P}{J}L_m i_{rq} & -\frac{3}{2}\frac{P}{J}L_m i_{rd} & 0 & 0 & -\frac{B}{J} \end{bmatrix} \quad (5)$$

where $i_{ds}$, $i_{qs}$, $i_{dr}$, $i_{qr}$ are the stator and rotor currents in the dq coordinate system, $\omega_r$ is the rotor angular speed, $V_{ds}$, and $V_{qs}$ are the control voltages applied to the stator, $L_s$, $L_r$, $R_s$, $R_r$, and $R_m$ are the electrical parameters of the IM, $L_m$ is the mutual inductance between the stator and rotor, $J$ and $B$ denote the moment of inertia and damping coefficient of the flywheel, respectively.

The matrix $A_1$ represents the variation of $A$ when considering the load fluctuation (affecting the rotor speed):

$$A_1 = \begin{bmatrix} 0 & 0 & 0 & 0 & \alpha \\ 0 & 0 & 0 & 0 & \beta \\ 0 & 0 & 0 & 0 & 0 \\ 0 & 0 & 0 & 0 & 0 \\ 0 & 0 & 0 & 0 & 0 \end{bmatrix} \quad (6)$$

where $\alpha$ and $\beta$ are the load-dependent coefficients.

The matrix $A_2$ represents the variation of $A$ when considering the magnetic saturation:

$$A_2 = \begin{bmatrix} 0 & 0 & -\frac{\gamma R_r}{L_s L_r} i_{rd} & -\frac{\delta R_r}{L_r L_r} i_{rq} & 0 \\ 0 & 0 & -\frac{\gamma R_r}{L_s L_r} i_{rd} & -\frac{\delta R_r}{L_s L_r} i_{rq} & 0 \\ \frac{\gamma R_s}{L_r} i_{rd} & \frac{\delta R_s}{L_s} i_{rq} & 0 & 0 & 0 \\ \frac{\gamma R_s}{L_r} i_{rd} & \frac{\delta R_s}{L_r} i_{rq} & 0 & 0 & 0 \\ 0 & 0 & 0 & 0 & 0 \end{bmatrix} \quad (7)$$

The elements in $A_2$ represent the effects of the magnetic saturation on the variations of the stator and rotor currents. The component $-\frac{\gamma R_r}{L_s L_r} i_{rd}$ in the first and second rows describes the influence of the rotor flux variation on the stator voltage, while the element $\frac{\gamma R_s}{L_r} i_{rd}$ in the third and fourth rows illustrates the impact of the magnetic saturation on the rotor current.

The matrix $A_3$ accounts for changes in $A$ when considering the parameter uncertainties. Assuming that the system parameters exhibit the uncertainties:

$$R_s = R_{s0}(1+\delta_1)$$
$$R_r = R_{r0}(1+\delta_2)$$
$$L_m = L_{m0}(1+\delta_3)$$
$$J = J_0(1+\delta_4)$$

$$A_3 = \begin{bmatrix} B & 0 & E & 0 & 0 \\ 0 & B & 0 & E & 0 \\ D & 0 & C & 0 & 0 \\ 0 & D & 0 & C & 0 \\ 0 & 0 & 0 & 0 & -\frac{\delta_4 B_0}{J_0} \end{bmatrix} \quad (8)$$

where $B = -\frac{\delta_1 R_{s0}}{L_s}$, $C = -\frac{\delta_2 R_{r0}}{L_r}$, $D = \frac{\delta_1 L_{m0}(1+\delta_3) R_{s0}}{L_r}$, $E = -\frac{\delta_2 L_{m0}(1+\delta_3) R_{r0}}{L_s L_r}$. The coefficient $\delta_1$ affects the stator resistance $R_s$, altering the decay rate of the stator current. The coefficient $\delta_2$ influences the rotor resistance $R_r$, impacting the rotor flux. The coefficient $\delta_3$ affects the magnetizing inductance $L_m$ modifying the coupling between the stator and rotor. The coefficient $\delta_4$ influences the moment of inertia $J$ altering the rotor speed dynamics $\omega_r$.

To control the flywheel rotational speed, and thereby regulate the power exchange with the grid, the relationship between the output power of FESS and the control signal can ideally be represented by a standard affine equation.

$$\dot{x} = f(x) + g(x)u$$

However, in practice, due to effects, such as magnetic saturation, time-varying parameters, and the inherently nonlinear and non-affine nature of the system, it cannot be expressed in a standard affine form. Instead, the system follows a generalized non-affine model:

$$\dot{x} = F(x,u) \quad (9)$$

where $x(t) = [i_{ds} \quad i_{qs} \quad i_{dr} \quad i_{dr} \quad \omega]^T$ represents the state variables, $u$ is the control input signal $u = [v_{sd} \quad v_{sq}]^T$, and $F(x,u)$ is a complex nonlinear function that cannot be decomposed into an affine form. To design the controller, the dynamic model of the IM-FESS system must be formulated in the dq reference frame.

The output power of the FESS is given by:

$$P_{out} = T_e \cdot \omega_r \quad (10)$$

where $T_e$ is the electromagnetic torque of the IM.

The above model highlights the system's strong nonlinearity and non-affine nature, making traditional control methods difficult to apply. To address these challenges, this study proposes an adaptive optimal tracking control method that does not require an explicit system model. This approach leverages a DNN identifier to identify the system dynamics and a CNN to optimize the control signal. By doing so, the control system can learn and adapt in real-time without needing an accurate mathematical model of the FESS.

## III. IM-FESS CONTROL DESIGN

### A. Proposed Control Scheme

The proposed control scheme is illustrated in Figure 2 and consists of the following main components:

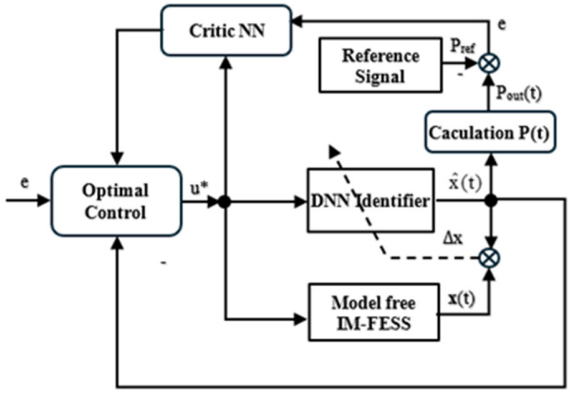


Fig. 2. Block diagram of the IM-FESS system.

- Optimal control: Generates the control signal $u$ to adjust the speed and torque of the IM to achieve the desired power output.
- CNN: Evaluates the control performance and optimizes the control signal $u$.
- Reference signal: Describes the desired response of the system.
- DNN identifier: Uses a dynamic DNN to learn the dynamics of the IM-FESS system in real time without requiring an accurate mathematical model.
- Model-free FESS: Simulates the actual system without requiring precise parameter information.
- Error signal ($e$) and state deviation ($\Delta x$): Reflects the difference between the actual and desired outputs, which are used for adjustments.

The proposed system utilizes a DNN to identify the FESS system in real time. The DNN learns the dynamics of the IM-FESS system by observing the input signal $u$ and the system's feedback signal. This allows the controller to adapt to the system variations without needing a predefined exact model. The optimal controller utilizes the identification signals from the DNN combined with the CNN to continuously update the control signal $u$, ensuring that the output power $P_{out}(t)$ optimally follows the reference power $P_{ref}(t)$.

### B. DNN Identifier Block

The neural network identifier predicts the state of the IM-FESS system based on previous input data. The use of DNN for the identification problem includes determining the inputs and outputs of the model, selecting the structure and activation function, and training, evaluating, and fine-tuning the model. The IM-FESS system is a highly complex nonlinear system influenced by various dynamic factors. Traditional Recurrent

Neural Networks (RNNs) often struggle with the vanishing gradient problem when handling long time-series data. Long Short-Term Memory (LSTM), a variant of RNN, effectively retains long-term dependencies, making it well-suited for modeling system dynamics.

This study employed an LSTM network, where the input $\hat{x}(t) = [i_{ds}, i_{qs}, i_{dr}, i_{qr}, \omega_r]^T [i_{ds}, i_{qs}, i_{dr}, i_{qr}, \omega_r, u^*]$ consists of past states, and the output is the predicted state. The network consisted of three LSTM layers, followed by a fully connected output layer. The number of neurons in each layer was 64 neurons in the first and second LSTM layers, and 32 neurons in the third LSTM layer (adjustable for performance optimization). The fully connected layer served as the final layer, with the function of receiving a feature vector (of size 32) from the last LSTM layer. The former transforms this vector into five outputs, corresponding to the five states of the IM-FESS system.

The activation function used was the *tanh* function. The optimization algorithm was the Adaptive Moment Estimation (Adam) with a learning rate of 0.001, batch size of 32, and 500 epochs.

The LSTM network was continuously updated using real-time data from the IM-FESS system. At each time *t*, the error value $\Delta x = x(t) - \hat{x}(t)$ is computed and is used to adjust the network's weights, employing the Adam optimization algorithm.

### C. Optimal Control Block for IM-FESS

In the control diagram, the optimal control block plays a critical role in ensuring that the FESS output power follows the reference power optimally, even in the absence of an accurate system model. This is achieved using adaptive control based on Reinforcement Learning (RL). The IM-FESS system state is defined as:

$$x = [i_{ds} \quad i_{qs} \quad i_{dr} \quad i_{qr} \quad \omega_r]^T$$

Find the control signal $u*$ to minimize the error between the actual power *P(t)* and the reference power $P_{ref}$:

$$e(t) = P_{ref} - P_{actual}(t) \tag{11}$$

The optimal objective function is formulated as an energy optimization problem:

$$J = \int_0^T [e^2 + \lambda u^2] dt \tag{12}$$

where $e^2$ is the power error component ensuring the tracking of $P_{ref}$, $\lambda u^2$ is the term that limits the excessive control signals ensuring system smoothness, and $T$ is the optimization time horizon.

The objective is to find a $u^*$ such that $\min_u J$.

### D. Some Common Mistakes

In optimal control, CNN plays a crucial role in evaluating the cost function or value function of the system. Common types of CNN include Value Function Approximation Critic (VFA-Critic), Hamilton-Jacobi-Bellman (HJB) Critic, Q-Learning Based Critic (Q-Critic), Advantage Actor-Critic (A2C/A3C) Critic, and Policy Evaluation Critic [11, 12].

In this paper, the HJB CNN was used to approximate the value function $J(x)$ and update it according to the HJB equation.

The CNN learns the value function $J(x)$ through a DNN $J(x, W_c)$ with weight parameter $W_c$. The input is the system state $x(t)$, hidden layers use the nonlinear activation function *tanh*, and the output is the cost function value $J(x)$. This network is trained to ensure that $J(x)$ satisfies the HJB equation:

$$\min_u \left[\frac{\partial J}{\partial x} f(x,u) + L(x,u)\right] = 0 \tag{13}$$

where $\Delta_i$ is the uncertainty matrix, $L(x,u)$ is the instantaneous cost function, $f(x,u)$ represents the state equations of the IM-FESS system, and $\partial J/\partial x$ is the gradient of the value function estimated by the CNN.

The training process of the CNN can be performed using Gradient Descent with derivatives concerning the weight parameter $W_c$:

$$\Delta W_c = -\eta_c \frac{\partial}{\partial W_c} \left[\frac{\partial J}{\partial x} f(x,u) + L(x,u)\right]^2$$

where $\eta_c$ is the learning rate of the CNN. The gradient of $J(x)$ can be computed using automatic differentiation.

This paper used an LSTM network with two inputs ($e$ and $u$), a first hidden layer with 40 neurons, a second hidden layer with 40 neurons, and an output representing the cost function value. The Gradient Descent learning algorithm was utilized. The training process of the CNN in Adaptive Dynamic Programmin (ADP) consists of the following steps:

- Step 1: Initialize the CNN with random weights $W_c$.
- Step 2: Obtain the current state $x(t)$ from the system.
- Step 3: Compute the gradient $\frac{\partial J}{\partial x}$ from CNN.
- Step 4: Compute the HJB error:

$$\mathcal{L}_{HJB} = \left(\frac{\partial J}{\partial x} f(x,u) + L(x,u)\right)^2$$

- Step 5: Update the weights $W_c$ of the CNN using Gradient Descent.
- Step 6: Repeat from Step 2 until convergence is achieved.

### E. Stability Analysis of the System

In the model-free IM-FESS system, the state matrix $A$ may vary due to disturbances, nonlinearities, fluctuating loads, and identification errors. To ensure stability for all possible values of $A$, the Linear Matrix Inequality (LMI) approach was applied, with uncertainties based on the Lyapunov condition.

The state matrix $A$ is represented as:

$$A = A_0 + \sum_{i=1}^{m} \Delta_i A_i, \quad \Delta_i \leq 1$$

where $A_0$ is the nominal matrix, $A_i$ represents the variation levels, and $\Delta_i$ is the uncertainty matrix.

The system is stable if there is a Lyapunov matrix $P > 0$ that satisfies the inequality:

$$A_0^T P + P A_0 + \sum_{i=1}^{m} |A_i^T P + P A_i| < 0$$

This LMI problem was solved using the YALMIP + SeDuMi tool in MATLAB. The simulation results confirm that the system meets stability conditions with a positive definite $P$, verifying the robustness of the proposed controller.

## IV. SIMULATION RESULTS AND DISCUSSION

The simulations were conducted in MATLAB using the FESS system parameters listed in Table I.

TABLE I. SIMULATION PARAMETERS

| Parameter | Value | Unit |
|---|---|---|
| Rated power | 50 | kW |
| Number of pole pairs (p) | 2 | |
| Flywheel inertia | 10.5 | kg·m² |
| Stator resistance $R_s$ | 0.05 | Ω |
| Stator inductance $L_s$ | $40.7 \times 10^{-3}$ | H |
| Rotor resistance $R_r$ | 0.043 | Ω |
| Rotor inductance $L_r$ | $40.7 \times 10^{-3}$ | H |
| Mutual inductance $L_m$ | 0.85 | Wb |
| Friction coefficient $B$ | 0.002 | N·m·s |
| Reference power $P_{ref}(t)$ | 30sin(5πt) | kW |

The model-free system identification results using DNN are shown in Figures 3-6.

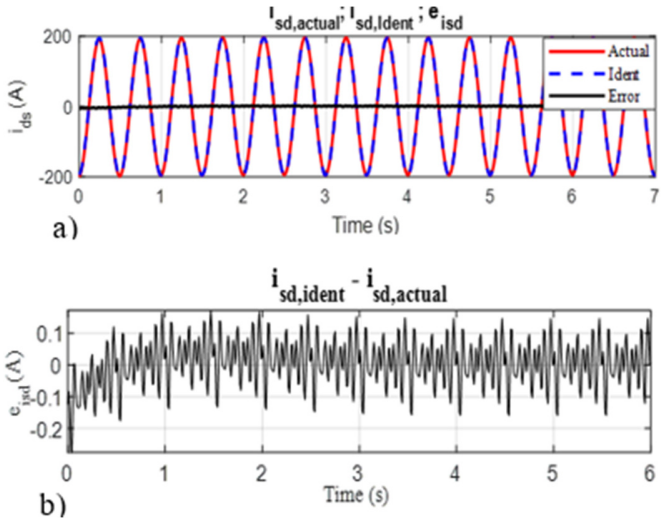


Fig. 3. The currents $i_{sd\_actual}$, $i_{sd\_ident}$, and $i_{sd\_actual}$ - $i_{sd\_ident}$.

Figures 3(a) and 4(a) depict the orthogonal components ($i_{sd}$, $i_{sq}$) of the FESS stator current, including the actual system current (solid red line), the online identified current using the DNN (dashed blue line), and the error between them (dashed black line). The error curves are shown in Figures 3(b) and 4(b). The maximum identification error was calculated as:

$$\Delta e_{i_s}\% = \frac{i_{s\_atual} - i_{s\_ident}}{i_{s\_actual}} 100\% \leq 0.1\% \qquad (15)$$

Figures 5(a) and 6(a) display the orthogonal components ($i_{rd}$, $i_{rq}$) of the FESS rotor current, including the actual system current (solid red line), the online identified current using the dynamic neural network (dashed blue line), and the error between them (dashed black line). The error curves are portrayed in Figures 5(b) and 6(b). The maximum identification error is:

$$\Delta e_{i_r}\% = \frac{i_{r\_actual} - i_{r\_ident}}{i_{r\_actual}} 100\% \leq 0.1\% \qquad (16)$$

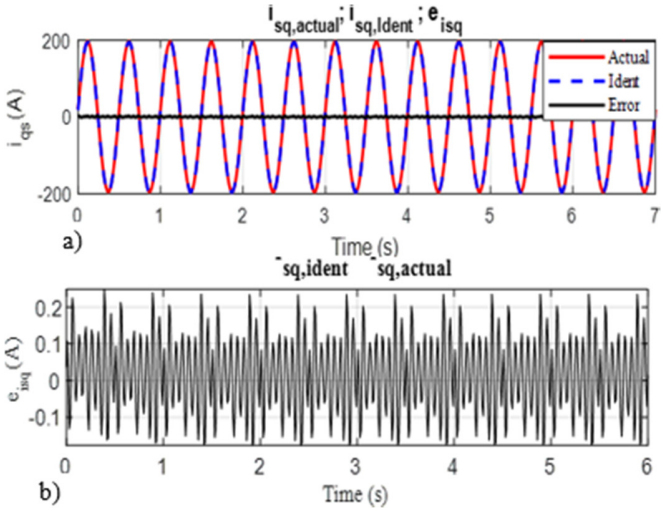


Fig. 4. The currents $i_{sq\_actual}$, $i_{sq\_ident}$ and $i_{sq\_actual}$ - $i_{sq\_ident}$.

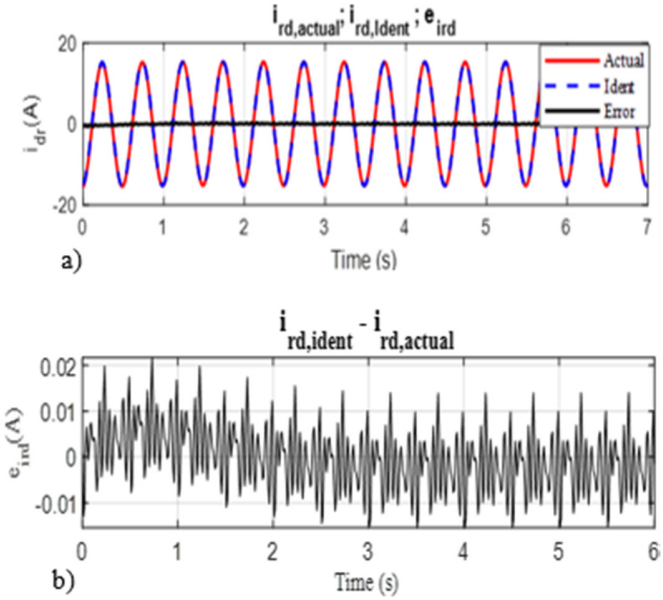


Fig. 5. The currents $i_{rd\_actual}$, $i_{rd\_ident}$ and $i_{rd\_actual}$ - $i_{rd\_ident}$.

The speed curves are shown in Figure 7a, and the identification errors are illustrated in Figure 7b. The maximum identification error is:

$$\Delta e_{\omega}\% = \frac{i_{\omega\_actual} - i_{\omega\_ident}}{i_{\omega\_actual}} 100\% \leq 0.01\% \qquad (17)$$

Figure 8(a) demonstrates the reference power and actual power of the IM-FESS over a 3-second simulation period with

the nominal parameters of the IM-FESS. The maximum tracking error is 0.03 kW, or:

$$\Delta P\% = \frac{P_{ref} - P_{FESS}}{P_{ref}} 100\% = \frac{0.03}{50} 100\% \leq 0.06\% \quad (18)$$

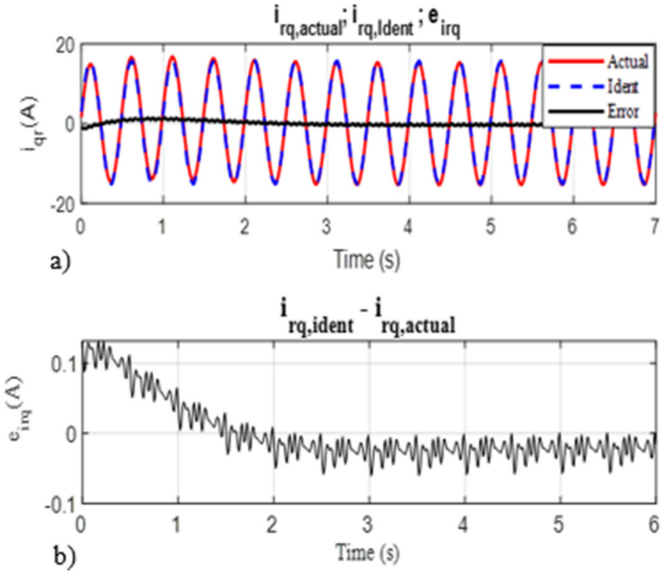


Fig. 6. The currents $i_{rq\_actual}$, $i_{rq\_ident}$ and $i_{rq\_actual}$ - $i_{rq\_ident}$.

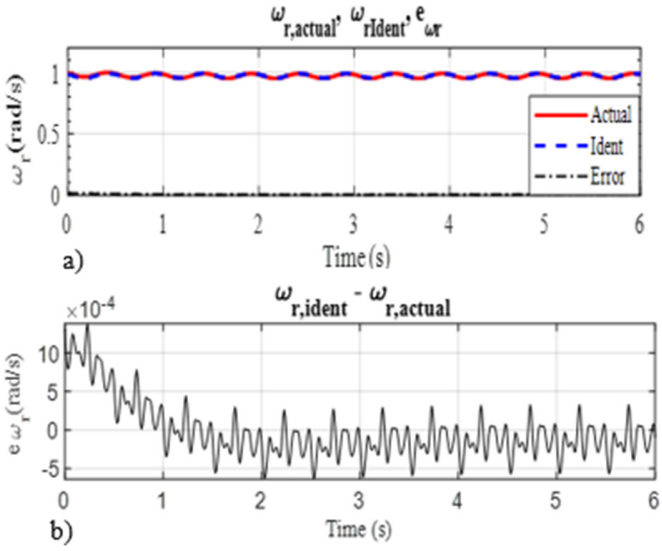


Fig. 7. Angular speeds $\omega_{r\_actual}$, $\omega_{r\_ident}$ and $\omega_{r\_actual}$, - $\omega_{r\_ident}$.

To evaluate the reference tracking performance of the proposed control method, simulations were conducted under the following assumptions: the load variations cause the system's moment of inertia to fluctuate by ±5%, the magnetic saturation leads to a 6% reduction in inductances ($L_s$, $L_r$, and $L_m$), and the parameter uncertainty due to temperature changes results in a 5% increase in the stator and rotor resistances.

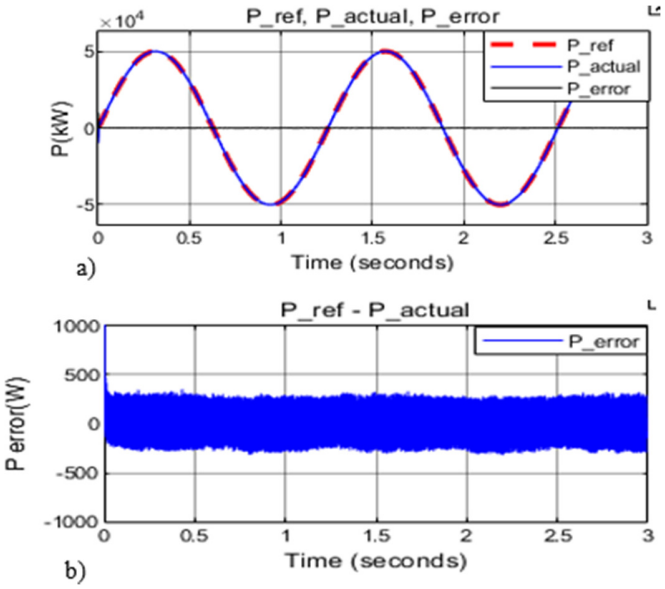


Fig. 8. a) Actual power and reference power curves, b) power error.

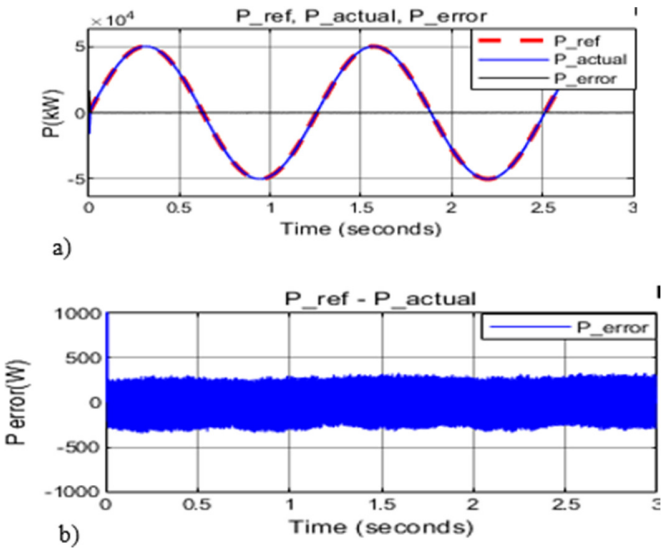


Fig. 9. a) Actual power and reference power curves considering load variation, magnetic saturation, and parameter uncertainty, b) power tracking error.

The simulation results displayed in Figure 9 indicate that the actual power curve continues to track the reference power with minimal tracking error variations. The *P_actual* curves in Figures 8 and 9 differ only in the initial transient phase.

## V. CONCLUSIONS

This paper proposes an adaptive optimal tracking control method that does not require a mathematical model of the system for a Flywheel Energy Storage System (FESS) based on an Induction Machine (IM). A Deep Neural Network (DNN) is employed to identify the nonlinear and uncertain dynamics of the IM-FESS in real-time. The proposed control strategy is designed to optimize the power response of the IM-FESS,

ensuring that the output power closely tracks the reference power signal with a minimal tracking error.

Compared to conventional model-based control methods, such as PID control, state feedback control, nonlinear backstepping control, or model predictive control, which typically require accurate system parameters and may perform poorly under uncertain conditions, the proposed method eliminates the dependence on the system model and demonstrates robustness against the load variations and external disturbances. Unlike traditional optimal controllers, the proposed DNN-based identification structure continuously learns and adapts its behavior, allowing it to maintain a high performance even under varying operating conditions. The simulation results show a superior tracking accuracy and disturbance rejection compared to the model-based approaches previously used in the literature [8-14], confirming the effectiveness of the proposed method.

The novelty of this work lies in the integration of model-free deep learning-based identification with adaptive optimal control in the context of FESS using an induction machine, a combination that has not been extensively explored in prior research. This contributes to the existing body of knowledge by providing a practical and scalable control solution for energy storage systems in smart grids.

Future research will focus on implementing the control system on real-time embedded hardware to validate its effectiveness under practical conditions. Furthermore, the approach will be extended by incorporating advanced deep learning techniques, such as deep reinforcement learning, to further enhance the system's adaptability and decision-making capabilities in dynamic and uncertain environments.

## ACKNOWLEDGEMENTS

The authors wish to thank the Thai Nguyen University of Technology for supporting this work.

## REFERENCES

[1] J. W. Zhang, Y. H. Wang, G. C. Liu, and G. Z. Tian, "A review of control strategies for flywheel energy storage system and a case study with matrix converter," *Energy Reports*, vol. 8, pp. 3948–3963, Nov. 2022, https://doi.org/10.1016/j.egyr.2022.03.009.

[2] M. E. Amiryar and K. R. Pullen, "A Review of Flywheel Energy Storage System Technologies and Their Applications," *Applied Sciences*, vol. 7, no. 3, Mar. 2017, Art. no. 286, https://doi.org/10.3390/app7030286.

[3] P. Tiwari, A. Kafle, P. Bijukchhe, and A. Bhattarai, "A review on Energy Storage Systems," *Journal of Physics: Conference Series*, vol. 2629, no. 1, Nov. 2023, Art. no. 012024, https://doi.org/10.1088/1742-6596/2629/1/012024.

[4] K. Xu, Y. Guo, G. Lei, and J. Zhu, "A Review of Flywheel Energy Storage System Technologies," *Energies*, vol. 16, no. 18, Jan. 2023, Art. no. 6462, https://doi.org/10.3390/en16186462.

[5] W. Su, T. Jin, and S. Wang, "Modeling and simulation of short-term energy storage: Flywheel," in *2010 International Conference on Advances in Energy Engineering*, Beijing, Jun. 2010, pp. 9–12, https://doi.org/10.1109/ICAEE.2010.5557629.

[6] A. Soomro, M. E. Amiryar, K. R. Pullen, and D. Nankoo, "Comparison of Performance and Controlling Schemes of Synchronous and Induction Machines Used in Flywheel Energy Storage Systems," *Energy Procedia*, vol. 151, pp. 100–110, Oct. 2018, https://doi.org/10.1016/j.egypro.2018.09.034.

[7] R. K. Miyamoto, A. Goedtel, and M. F. Castoldi, "A proposal for the improvement of electrical energy quality by energy storage in flywheels applied to synchronized grid generator systems," *International Journal of Electrical Power & Energy Systems*, vol. 118, Jun. 2020, Art. no. 105797, https://doi.org/10.1016/j.ijepes.2019.105797.

[8] G. O. Suvire and P. E. Mercado, "DSTATCOM with Flywheel Energy Storage System for wind energy applications: Control design and simulation," *Electric Power Systems Research*, vol. 80, no. 3, pp. 345–353, Mar. 2010, https://doi.org/10.1016/j.epsr.2009.09.020.

[9] S. Samineni, B. K. Johnson, H. L. Hess, and J. D. Law, "Modeling and analysis of a flywheel energy storage system for voltage sag correction," in *IEEE International Electric Machines and Drives Conference, 2003. IEMDC'03.*, Madison, WI, USA, Jun. 2003, vol. 3, pp. 1813–1818, https://doi.org/10.1109/IEMDC.2003.1210699.

[10] T. A. Theubou Tameghe, R. Wamkeue, and I. Kamwa, "Modelling and Simulation of a Flywheel Energy Storage System for Microgrids Power Plant Applications," presented at the EIC Climate Change Technology Conference 2015, Québec, Canada, 2015.

[11] A. Shahzad, S. Munshi, S. Azam, and M. Khan, "Design and Implementation of a State-feedback Controller Using LQR Technique," *Computers, Materials & Continua*, vol. 73, no. 2, pp. 2897–2911, 2022, https://doi.org/10.32604/cmc.2022.028441.

[12] S. Mensou, A. Essadki, I. Minka, T. Nasser, and B. B. Idrissi, "Backstepping Controller for a Variable Wind Speed Energy Conversion System Based on a DFIG," in *2017 International Renewable and Sustainable Energy Conference (IRSEC)*, Tangier, Morocco, Dec. 2017, pp. 1–6, https://doi.org/10.1109/IRSEC.2017.8477586.

[13] A. Bektache, H. Achouri, and K. S. Belkhir, "Robust Nonlinear Predictive Control Applied to Induction Motors," *Engineering, Technology & Applied Science Research*, vol. 13, no. 3, pp. 10951–10956, Jun. 2023, https://doi.org/10.48084/etasr.5732.

[14] H. Khechini and M. Gossa, "Fault tolerant robust control applied for induction motor (LMI approach)," *Journal of Electrical Systems*, vol. 3, no. 3, pp. 162–175, 2007.